GEOPHYSICAL RESEARCH LETTERS, VOL. 29, NO. 23, 2135, doi:10.1029/2002GL015562, 2002

Seismotomography of the crust in the transition zone between the southern Tyrrhenian and Sicilian tectonic domains

G. Neri,[1] G. Barberi,[2] B. Orecchio,[1] and M. Aloisi[2]

Received 29 May 2002; revised 21 September 2002; accepted 3 October 2002; published 13 December 2002.

[1] A crustal tomography of seismic wave velocity was performed in the contact zone between the southern Tyrrhenian, Sicilian and Ionian tectonic units, a zone where the lithospheric structure can be expected to furnish evident signatures of dynamics related to the Tyrrhenian subduction process. A dataset of 10241 P and 5597 S readings from 932 local earthquakes recorded between 1978 and 2001 by stations operating in Sicily and Calabria was inverted by the SIMULPS12 algorithm for simultaneous computation of hypocenter parameters and V_p and V_p/V_s three dimensional distributions. The study brought significant improvement in the knowledge of the local velocity structure, furnishing new information useful to better identify the local tectonic units. The results appear to be compatible with the most recent hypotheses regarding the geodynamics of the study region. *INDEX TERMS:* 7205 Seismology: Continental crust (1242); 7220 Seismology: Oceanic crust; 7203 Seismology: Body wave propagation; 8180 Tectonophysics: Evolution of the Earth: Tomography. **Citation:** Neri, G., G. Barberi, B. Orecchio, and M. Aloisi, Seismotomography of the crust in the transition zone between the southern Tyrrhenian and Sicilian tectonic domains, *Geophys. Res. Lett.*, *29*(23), 2135, doi:10.1029/2002GL015562, 2002.

1. Geodynamic Scenario of the Investigation

[2] Many investigators [see, among others, *Malinverno and Ryan*, 1986; *Faccenna et al.*, 1996 and 2001; *Argnani*, 2000; *Nicolich et al.*, 2000; *Doglioni et al.*, 2001; *Gvirtzman and Nur*, 2001] suggested that geological and geophysical evidences in the Southern Tyrrhenian region can be interpreted in the framework of a geodynamic model assuming southeastward rollback of a Ionian lithosphere slab subducting beneath the Tyrrhenian lithosphere (Figure 1). Rollback is widely believed to have been the primary tectonic source for (1) the southeastward kinematics of the southern Tyrrhenian lithosphere, (2) its thinning and overthrusting onto the Ionian lithosphere, and (3) the Tyrrhenian basin opening. On a smaller scale, Mt. Etna volcanic activity is interpreted as due to extensional processes occurring along the southwestern border of the rollbacked Ionian slab [*Gvirtzman and Nur*, 1999; *Nicolich et al.*, 2000; *Doglioni et al.*, 2001]. Strong lateral heterogeneity affects the lithosphere in this region [see e.g., *Scarpa*, 1982; *Panza et al.*, 1990; *Plomerova et al.*, 1998]. A major feature is high-gradient crustal thinning from inner lands of Sicily and Calabria to the Tyrrhenian and Ionian basins [Figure 2; *Dezes and Ziegler*, 2001] corresponding to notable increase in surface heat flow [*Mongelli et al.*, 1989] and gravity [*Catalano et al.*, 2001]. A system of strike-slip faults cuts the southern Tyrrhenian and Calabrian Arc lithosphere (Figure 1) and accommodates the ca. southeastward motion of the southern Tyrrhenian tectonic unit with respect to the units confining to northeast (Adriatic) and southwest (Sicily-Africa).

[3] Based on recent improvements of seismic monitoring and collection of new data in the southern Tyrrhenian region we propose here a seismic tomography that remarkably improves the knowledge of the local crust velocity structure. The information available in the literature in this regard comes from analyses of limited portions of few DSS profiles [see e.g., *Cernobori et al.*, 1996; *Nicolich et al.*, 2000] and tomographic investigations performed with data of earthquakes recorded before 1992 [*De Luca et al.*, 1997]. In the former case the information is partial, in the latter the resolution of velocity estimates is lower than achievable today. Improving the knowledge of the crustal velocity structure in this peculiar subduction zone will help future earthquake studies and is also expected to concur with upper mantle tomographic analyses by other investigators [*Piromallo and Morelli*, 1997; *Cimini*, 1999; *Lucente et al.*, 1999] to furnish an increasingly accurate picture of the local tectonic units and geodynamic processes.

2. Seismic Dataset and Tomographic Inversion

[4] We used for tomographic inversion P- and S-wave readings from local earthquakes recorded by seismic stations operating in Sicily and Calabria in the period January 1978 – March 2001. These data were furnished by *Istituto Nazionale di Geofisica e Vulcanologia* and the Cosenza, Messina and Catania universities. More than five thousand shallow events were located using the VELEST algorithm [*Kissling et al.*, 1994] and a 1D velocity model routinely used for hypocenter locations in the study region (Figure 3). In order to obtain a dataset suitable for tomography, we selected 932 of these events on the basis of (i) number and quality of readings, (ii) the distribution of recording stations around the epicenter, and (iii) hypocenter location quality. Figure 3 shows the P and S ray tracing obtained in the routine velocity model for the selected dataset and furnishes a first evidence that data are appropriate for investigating the 3D velocity structure in the area including northeastern Sicily, southern Calabria and the southeastern Tyrrhenian sea. Following *Kissling et al.* [1994], we first sought for the "minimum 1D model", i.e., the 1D velocity model that best describes the P-wave local propagation

[1]Dipartimento di Scienze della Terra, Messina University, Italy.
[2]Istituto Nazionale di Geofisica e Vulcanologia, Sezione di Catania, Italy.

0094-8276/02/2002GL015562$05.00

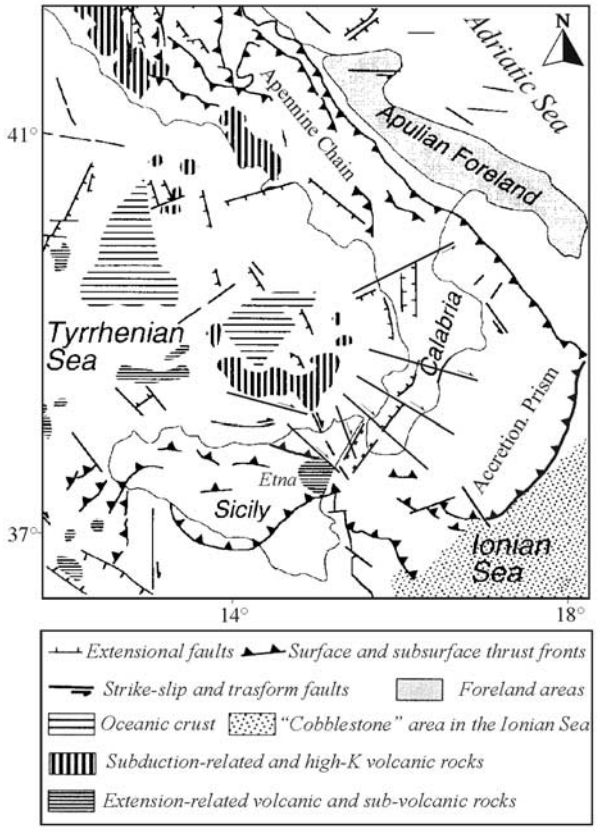

Figure 1. Structural map of the Tyrrhenian-Apennine domain [modified from *Faccenna et al.*, 1996].

features, to be used as starting model for 3D inversion. For this purpose, we performed by VELEST the 1D inversion of the phase readings relative to 500 events (the maximum allowed by the code) extracted from the selected dataset according to the criterion of satisfactorily covering the study volume. The routine model was used as starting model for the minimum 1D model computation. The minimum 1D model is reported in Figure 3 (continuous trace). Then, we used the SIMULPS12 algorithm [*Thurber*, 1983; as modified by *Thurber*, 1993 and *Eberhart-Phillips*, 1993] for 3D inversion. A preliminary choice of the grid structure needed by this algorithm was made on the basis of ray tracing obtained by the pseudo-bending raytracer [*Um and Thurber*, 1987] after location of the selected dataset (932 events) in the minimum 1D model. Refinements of the grid were made after investigations of the inversion matrix diagonal elements and Derivative Weight Sum, two markers of resolution level of velocity estimates at the grid nodes [*Haslinger et al.*, 1999]. The final grid chosen for tomography is reported in Figure 4a (depth levels 0, 6, 12, 18, 24 and 30 km). Velocity at the nodes indicated by full circles in this figure were fixed to values derived from DSS information available in the literature. The evaluation of the quality of the 3D model resulting from tomographic inversion was made by analyzing the Spread Function (SF) as defined by *Michelini and McEvilly* [1991]. On the basis of results from a series of synthetic tests, and referring also to other investigators' experience [see e.g., *Eberhart-Phillips and Michael*, 1998], we decided to use a SF upper bound of 4.0 for delimitating the zones of reliability of the model. Figures 4a–4f displays the V_p component of the model obtained by tomography (the V_s component is not reported for conciseness and because the S-wave velocity pattern is very similar to V_p's; $V_p/V_s = 1.75 \pm 0.04$). This 3D model marks a notable improvement respect to the minimum 1D model as regard to fitting of arrival times used for inversion, and this is evidenced by the clear drop from 0.35 to 0.21 sec of the arrival-time residual *rms*. Figure 4g shows one of the synthetic tests performed to evaluate if the inversion method and the dataset used for tomography are appropriate for reconstructing the crustal structure in the study area. This test was carried out as a typical restore test: (i) the theoretical arrival times were estimated in the velocity structure of Figures 4a–4f for all the hypocenter-station pairs of the dataset used for inversion; (ii) the obtained arrival times were randomly perturbed according to the experimental data uncertainty; (iii) the perturbed values were inverted for the 3D velocity structure. Figure 4g displays the P velocity distribution found with this procedure at the 0 km depth level: comparison with Figure 4a shows that the reconstruction of the original velocity pattern was satisfactory. Velocity distributions obtained by the test at the other depth levels (not reported here for

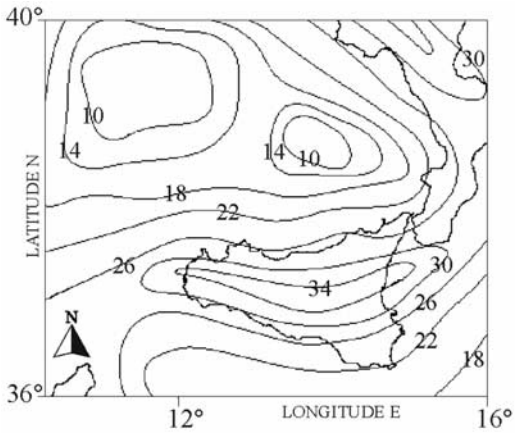

Figure 2. Isolines of the Moho depth (in km) redrawn from *Dezes and Ziegler* [2001].

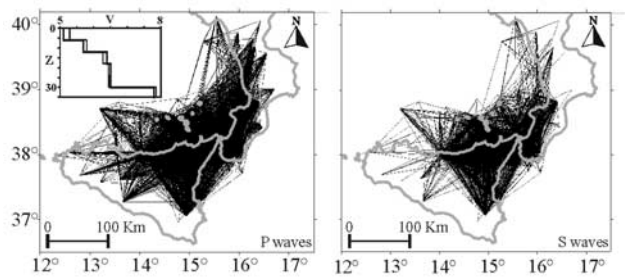

Figure 3. Ray tracing of P and S waves in the routine velocity model for the dataset selected for tomography. The routine model (dotted trace) and the minimum 1D model (continuous) are reported in the inset (V and Z stand for P velocity, km/s, and b.s.l. depth, km, respectively).

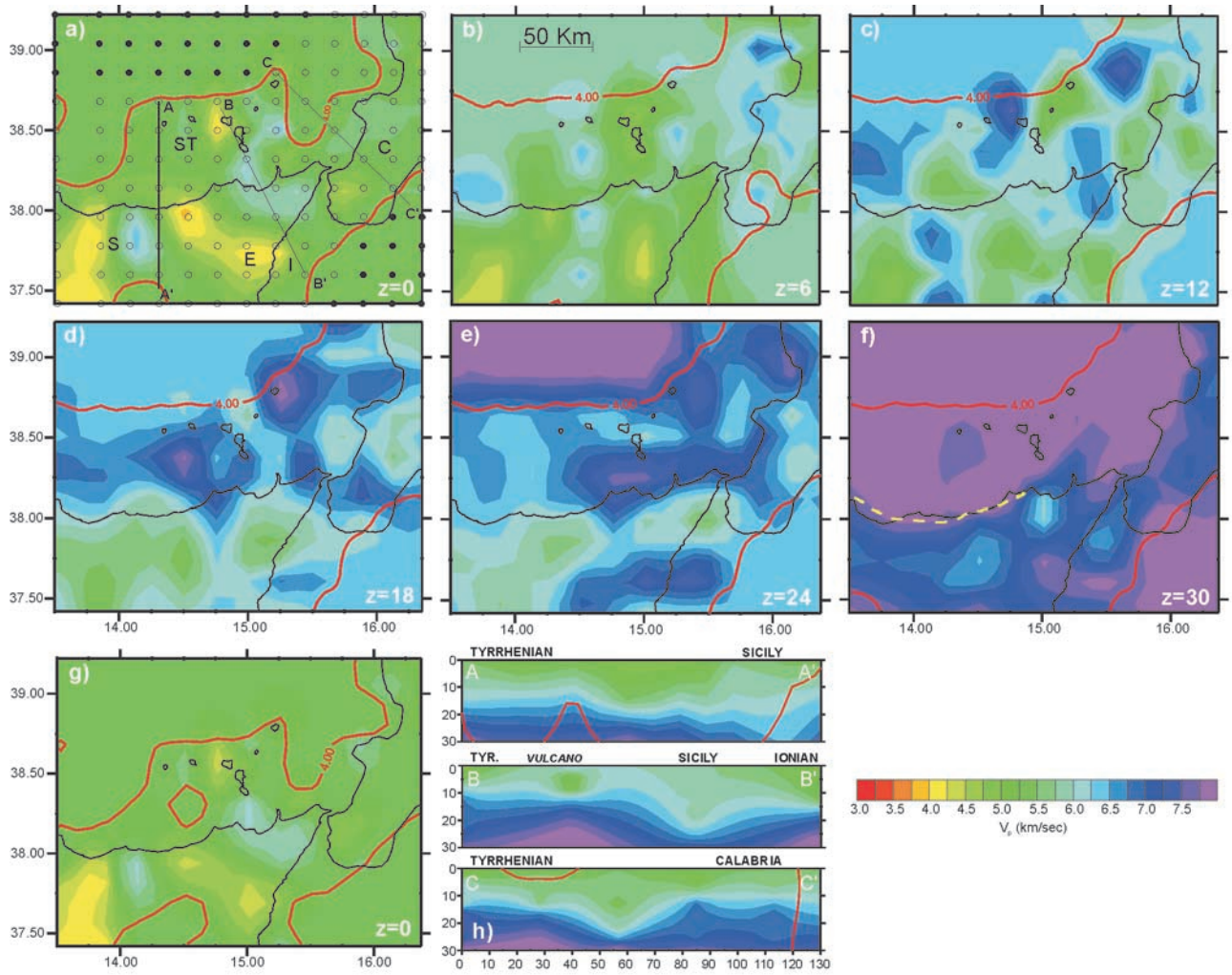

Figure 4. (a–f) P-wave velocity model obtained in the present study. Z is the b.s.l. depth in kilometers. The red curve contours the area where the Spread Function SF < 4.0. The dotted yellow curve in 4f indicates the separation between the Tyrrhenian and Sicilian velocity domains (see text). ST, S, E, I and C in 4a stand for Southern Tyrrhenian sea, Sicily, Etna, Ionian sea and Calabria, respectively. Again in 4a the circles indicate the nodes of the inversion grid (full circles mean fixed velocity values), and AA′, BB′ and CC′ are the profiles of the vertical sections given in 4h. (g) Results from the restore test described in the text. (h) Vertical sections of the 3D velocity model of 4a–f along the profiles AA′, BB′ and CC′ indicated in 4a.

conciseness) resulted also to be very similar to the original velocity distributions of Figures 4b–4f. Also, comparison of plates 4a and 4g shows that the SF = 4.0 curve contours reliability zones of the model. Finally, Figure 4h displays some vertical sections of the model represented in 4a–f.

3. Discussion of Results

[5] V_p and V_s distributions from the present tomographic investigation bring a significant improvement in the knowledge of the crustal structure in the study area. In comparison to the only shallow tomography previously carried out in the same area [*De Luca et al.*, 1997], we extended the dataset until doubling the number of phase readings and improved its overall quality by inclusion of data from earthquakes of the last nine years (1992 – March 2001): this allowed us to obtain greater resolution of velocity estimates and the enlargement of the study area. De Luca et al.'s main findings appear, however, to be confirmed by the present study. Our results can be summarized as follows.

[6] The dotted yellow curve in Figure 4f (depth level 30 km) marks the separation between a mantle velocity domain (V_p > 7.75 km/sec) to the north of the Tyrrhenian coast of Sicily and a crustal domain to the south. The crustal domain beneath Sicily continues beneath southern Calabria. The 30 km isobath of the Moho roughly runs along the northern coast of Sicily and the western coast of Calabria. A certain difference can be observed by comparing this data with the information available in the literature (Figure 2). It has to be considered that the pattern of Figure 2 comes from averaging the data on a larger scale than in our tomography. A general correspondence exists between the 30 km isobath trend inferred from data of Figure 4f and the Bouguer anomaly pattern [*Catalano et al.*, 2001]. A noteworthy feature in the map of Figure 4f is represented by mantle velocity found at the same depth level beneath eastern Etna

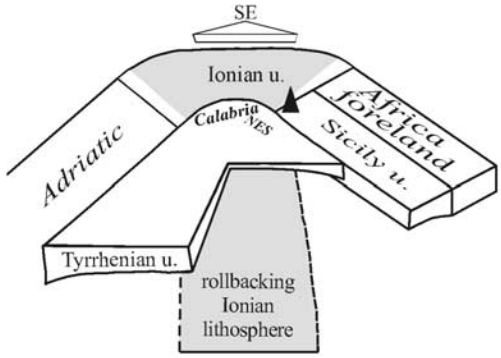

Figure 5. Sketch representation of the tectonic units in the study region. NES = Northeastern Sicily. The dark area indicates the rollbacking portion of the subduction structure. The triangle marks the Etna location. Lithosphere thinning can be noted northwest of the rollbacking slab.

and the confining Ionian area. Crustal thinning was evidenced by previous investigators in this area [see e.g., *Nicolich et al.*, 2000]. Finally, relatively low velocity values are found at the same depth level beneath central Sicily, in agreement with crustal thickening and a major negative Bouguer anomaly evidenced by all the previous investigators in the same area.

[7] Transition from a high-velocity Tyrrhenian domain to a low-velocity Sicilian one can also be observed at the depths of 24 and 18 km (Figures 4e–4d), and yet again roughly corresponds with the northern coast of Sicily. Noteworthy high-velocity zones appear beneath Calabria (Figures 4e–4d). Low velocity beneath central Sicily and high velocity beneath Etna-Ionian detected at the 30 km depth level are still present at the levels 24 and 18 km but high velocity tends to disappear at the 18 km depth level (Figure 4d).

[8] The presence of two distinct velocity domains (Tyrrhenian and Sicilian) tends to disappear in the upper crust (depth levels 12, 6 and 0 km, Figures 4c–4b–4a), even if the average velocity value beneath the Tyrrhenian area is still greater than beneath Sicily. The low velocity zone found at deeper depths beneath central Sicily has in part vanished (Figures 4c–4b–4a), the high velocity zone beneath Etna-Ionian has practically disappeared.

[9] The vertical sections reported in Figure 4h evidence the crustal thinning from the inner lands of Sicily and Calabria to the Tyrrhenian and Ionian basins. Also, a minimum of crustal thickness can be noted beneath Vulcano island (section BB′) and this indicates the opportunity of more detailed investigations in that sector in the near future using also data from the local volcanological network. Another interesting feature is the remarkable thickness of the lower-crust velocity domain beneath Calabria (CC′).

[10] Tomographic results are compatible with the regional geodynamic model according to which the SE-ward rollback of a Ionian subducting slab has determined lithosphere thinning northwest of the slab, with greatest effects beneath the southern Tyrrhenian sea (Figure 5). This model explains the clear velocity change detected by tomography at depths deeper than 18 km beneath the northern coast of Sicily (transition from the Sicilian crustal domain to the Tyrrhenian mantle domain) as well as the attenuated evidence of the change at shallower depths (0, 6 and 12 km; transition from the Sicilian to the Tyrrhenian crust). Underthrusting of the Ionian domain below Calabria (Figure 5) may explain low velocity values found at the depth of 30 km beneath Calabria (crustal rocks of the Ionian slab) and the generally high values at shallower levels in the same area (Tyrrhenian unit). As well, crust extension-thinning and mantle upwarping related with the dynamics at the southwestern border of the rollbacked slab [*Gvirtzman and Nur*, 1999; *Nicolich et al.*, 2000; see also Figure 5] may justify high velocity we found at the depth levels 24 and 30 km beneath Etna-Ionian. Tomographic signatures of transitions between the Sicilian (S), Tyrrhenian (T) and Ionian (I) tectonic units (Figures 4 and 5) can be identified beneath the northern coast of Sicily (T-S), at a depth of 20–25 km beneath Calabria (T-I), and in the Etna area (S-I).

[11] **Acknowledgments.** The present work was supported by *Istituto Nazionale di Geofisica e Vulcanologia* in the framework of a collaboration agreement between INGV and Messina University.

References

Argnani, A., *Ann. Geofis.*, *43*(3), 585–607, 2000.
Catalano, R., et al., *Geophys. J. Int.*, *144*(1), 49–64, 2001.
Cernobori, L., et al., *Tectonophysics*, *264*, 175–189, 1996.
Cimini, G., *Geophys. Res. Letters*, *26*(24), 3709–3712, 1999.
De Luca, G., et al., *Phys. Earth Planet. Inter.*, *103*, 117–133, 1997.
Dezes, P., and P. A. Ziegler, *2nd EUCOR-URGENT Workshop*, Mt. St. Odile, France, 2001.
Doglioni, C., et al., *Terra Nova*, *13*(1), 25–31, 2001.
Eberhart-Phillips, D., *Seismic Tomography*, *Chapman & Hall*, *London*, 613–643, 1993.
Eberhart-Phillips, D., and A. J. Michael, *JGR*, *103*, 21,099–21,120, 1998.
Faccenna, C., et al., *Geophys. J. Int.*, *126*, 781–795, 1996.
Faccenna, C., et al., *Earth Planet. Sci. Lett.*, *187*, 105–116, 2001.
Gvirtzman, Z., and A. Nur, *Nature*, *401*, 782–785, 1999.
Gvirtzman, Z., and A. Nur, *Earth Planet. Sci. Lett.*, *187*, 117–130, 2001.
Haslinger, F., et al., *Tectonophysics*, *304*(3), 201–218, 1999.
Kissling, E., et al., *JGR*, *99*, 19,635–19,646, 1994.
Lucente, F. P., et al., *JGR*, *104*(B9), 20,307–20,327, 1999.
Malinverno, A., and W. B. F. Ryan, *Tectonics*, *5*(2), 227–245, 1986.
Michelini, A., and T. V. McEvilly, *BSSA*, *81*, 524–552, 1991.
Mongelli, F., et al., *Tectonophysics*, *164*, 267–280, 1989.
Nicolich, R., et al., *Tectonophysics*, *329*, 121–139, 2000.
Panza, G. F., et al., *J. Geodyn.*, *12*, 189–215, 1990.
Piromallo, C., and A. Morelli, *Ann. Geofis.*, *40*(4), 963–979, 1997.
Plomerova, J., et al., *Ann. Geofis.*, *41*(1), 33–48, 1998.
Scarpa, R., *Pure and Appl. Geophys*, *120*, 583–606, 1982.
Thurber, C., *JGR*, *88*, 8226–8236, 1983.
Thurber, C., *Seismic Tomography*, *Chapman & Hall*, *London*, 1993.
Um, J., and C. Thurber, *BSSA*, *77*, 972–986, 1987.

M. Aloisi and G. Barberi, I.N.G.V., Catania, Italy.
G. Neri and B. Orecchio, Messina University, Italy.